ARTICLE

PDLIM2 prevents the malignant phenotype of hepatocellular carcinoma cells by negatively regulating β-catenin

Xiaoming Jiang[1,2] · Zhe Chu[1,2] · Yang Cao[1] · Ying Tang[3] · Ying Shi [4] · Xu Shi [1]

Abstract

Hepatocellular carcinoma (HCC) is one of the most common malignancies and leading causes of cancer-related deaths globally. Despite significant advances in therapy, the molecular mechanisms underlying HCC development and progression remain unclear. Here, we aimed to explore the potential role of PDLIM2 in the development and epithelial-mesenchymal transition (EMT) of HCC *via* a possible modulation of β-catenin. We first confirmed that PDLIM2 was downregulated in HCC tissues and cells and found lower PDLIM2 expression was associated with worse prognosis in HCC patients. Loss- and gain- of function experiments were performed to evaluate the roles of PDLIM2 and β-catenin in HCC cell proliferation, migration, invasion, EMT, and colony formation. EMT was determined based on the levels of E-cadherin, zonula occludens-1, N-cadherin, and vimentin expression. In vivo, the roles of PDLIM2 and β-catenin in HCC were investigated by using a nude mouse xenograft model. It should be noted that PDLIM2 led to the inhibition of β-catenin activity and its downstream gene expression. Importantly, ectopic PDLIM2 expression inhibited the proliferation, migration, invasion, and EMT of HCC cells by reducing β-catenin expression both in vitro and in vivo, thereby suppressing the occurrence and progression of HCC. Taken together, our results demonstrated that overexpressed PDLIM2 exerts a tumor-suppressive role in HCC by regulating β-catenin. This study suggests that the PDLIM2 may be a promising target for the treatment of HCC.

Introduction

Hepatocellular carcinoma (HCC) is a heterogeneous and invasive malignant tumor, originating from a single tumor cell, where sequential genomic and epigenomic events result in significant diversity of HCC tumor cells [1]. While advances have been made in diagnosis, surgical, chemical therapy, and molecular targeted therapies, the recurrence and metastasis in HCC remains high and the 5-year survival rate is yet unsatisfactory [2]. Epithelial-mesenchymal transition (EMT) is a process in which epithelial cells acquire a mesenchymal phenotype and is a critical event in the metastasis of several tumors including HCC [3]. Accumulating evidence has highlighted potential novel molecular biomarkers and targets in HCC, which may be targeted for new diagnostics and drug development, particularly for identifying and treating metastatic events [4]. Specific proteins are understood to influence the tumor microenvironment and govern cancer cell phenotypes, and thus their identification can expand the understanding of HCC pathogenesis [5].

PDLIM2 (also known as slim 15 or mystiq16) is a nuclear protein, which belongs to a large family of LIM proteins consisting of two domains, including PDZ (postsynaptic density 65-discs large-zonula occludens 1) and LIM (abnormal cell lineage 11-islet 1-mechanosensory abnormal 3) [6]. A recent study has demonstrated that PDLIM2 expression is epigenetically repressed in multiple human cancer types [7]. Deregulated

These authors contributed equally: Xiaoming Jiang, Zhe Chu

Supplementary information The online version of this article (https://doi.org/10.1038/s41417-020-00257-6) contains supplementary material, which is available to authorized users.

✉ Ying Shi
 shiyingjlu@163.com

✉ Xu Shi
 shixu@jlu.edu.cn

1 Clinical Laboratory, the First Hospital of Jilin University, Changchun 130000, China

2 Department of Emergency, the First Hospital of Jilin University, Changchun 130000, China

3 Department of Respiration, the First Hospital of Jilin University, Changchun 130000, China

4 Department of Hepatology, Medical School of Jilin University, Changchun 130000, China

PDLIM2 has been implicated in the tumorigenesis of several tumors such as colorectal cancer and colon cancer [8, 9], while its putative role in HCC remains to be defined. In HCC, β-catenin has been found to be associated with tumor progression and worse prognosis [10]. β-catenin may subsequently be degraded or transferred to the nucleus, consequently regulating the expression of downstream genes [11]. Dysregulated β-catenin signaling is found in 30–40% of human HCC, mainly owing to mutations in β-catenin, and the Wnt/β-catenin pathway has been specifically implicated in HCC progression [12]. Notably, β-catenin is known to serve as a regulator of EMT processes in HCC [13]. In the present study, we hypothesized that PDLIM2 may influence the malignant phenotype of HCC cells by regulating β-catenin activity.

Materials & methods

Ethics statement

Ethical approval for the use of human specimens was obtained from the Research Ethics Committee of the First Hospital of Jilin University. All patients provided written informed consent. The study protocol was in accordance with the ethical standards formulated in the *Helsinki Declaration*. Animal experiments were conducted in strict accordance with the Guide for the Care and Use of Laboratory Animals published by the US National Institutes of Health. Great efforts were made to minimize the number of animals used in the experiments and their suffering. The animal experiment protocols were approved by the Ethics Committee of the First Hospital of Jilin University.

Microarray analysis

HCC and normal liver tissue-related microarray data GSE45267 was obtained from the Gene Expression Omnibus database (https://www.ncbi.nlm.nih.gov/geo/). The R package "limma was applied for differential gene expression analysis of the microarray data and a volcano map was drawn. The PDLIM2 gene was screened, and the 'Oncomine' web-based resource was used to analyze the difference in its expression level between HCC and normal liver tissues. Kaplan–Meier analysis was performed to analyze the relationship of PDLIM2 expression with overall survival and disease recurrence in HCC patients.

Clinical specimens

A total of 42 HCC tissue samples confirmed by pathological examination were collected from HCC patients (29 males and 13 females, aged from 40 to 72 years old, with a median age of 52 years old), who underwent hepatic carcinectomy between 2008 and 2013 at the First Hospital of Jilin University. None of the included patients had received any preoperative treatments prior to enrollment such as radiofrequency ablation, transcatheter arterial chemoembolization, immunotherapy, or targeted therapy. All the tumor nodules were completely removed and confirmed by pathological examination to ensure all the tumor tissues on the surface were excised. Complete clinicopathological and follow-up data were provided. Patients who died from non-liver diseases or accidents were excluded from the study. Another 18 cases of normal liver tissues were obtained from healthy donors of liver transplantation. The tissues were preserved in liquid nitrogen immediately after resection. A part of the tissue was used for Western blot analysis. Remaining tissues were used for immunohistochemical staining after preservation, formalin fixation, and paraffin-embedding.

Cell culture

The human immortalized normal hepatocyte cell line HL7702 (L02) and HCC cell lines SMMC7721, MHCC97L, Huh7, SMMC7721, SK-Hep1, HCCLM3, and MHCC97H were purchased from American Type Culture Collection (Manassas, VA, USA). Cells were cultured at 37 °C with 5% CO_2 in Dulbecco's modified Eagle's medium (DMEM) (Thermo Fisher Scientific Inc., Waltham, MA, USA) supplemented with 10% fetal bovine serum (FBS) (Gibco, Rockville, MD, USA).

Immunohistochemistry

The samples were fixed with 4% formaldehyde, followed by paraffin embedding, conventional dewaxing, gradient ethanol hydration, antigen retrieval under high pressure, antigen sealing, and incubation with a working solution of the primary antibody 37 °C for 1 h. After a wash with phosphate-buffered saline (PBS), mouse secondary antibody (Cat: 8125, Cell Signaling Technology [CST], Beverly, MA, USA) was added and incubated with the samples at room temperature for 30 min. The color was visualized with diaminobenzine (Sigma-Aldrich Chemical Company, St Louis, MO, USA). Then the samples were counterstained with hematoxylin, dehydrated, and mounted. Subsequently, the samples were incubated with the following antibodies, PDLIM2 (1:100, ab119243, Abcam Inc., Cambridge, MA, USA) and β-catenin (1:200, ab32572, Abcam) with PBS serving as a negative control (NC). The images were observed and analyzed under an optical microscope. Five high-power fields were randomly selected from each section with 100 cells per field. The images were analyzed using Image-ProPlus software (Version4.1) (MediaCybernetics, Maryland, USA) by 2 persons who were blinded to the experimental groups. Based on the percentage of positive

staining tumor cells, a threshold of positive tumor cells/all tumor cells > 10% was regarded as positive (+) and ≤ 10% as negative (−).

Cell transfection

HCC cells in the logarithmic growth phase were inoculated into a 6-well plate (4×10^5 cells/well). When the cells confluence reached 70–80%, the cells were transfected using Lipofectamine 2000 reagents according to manufacturer's instructions. Once the best site for knockdown of PDLIM2 was identified, the cells were transfected with short hairpin RNA (shRNA) targeting PDLIM2 (sh-PDLIM2), overexpression (oe)-PDLIM2, and shRNA targeting β-catenin (sh-β-catenin) plasmids. The sh-NC, oe-NC, and sh-PDLIM2 + sh-NC plasmids served as NC. All plasmids were provided by the Tianjing WOSUNBIO Co., Ltd. (Tianjing, China). After transfection for 6–8 h, the medium was renewed. The transfection efficiency was observed under the microscope (Leica DM1600B, Leica, Wetzlar, German) at 48 h after transfection, and the cells were cultured for subsequent experiments

Wound healing assay

Cells were cultured in a 6-well plate and grown to 95% confluence. The bottom of the well was scratched with a 10-µL pipette tip. Images were captured at 0 h and 24 h under an inverted microscope and the cell migration rate was calculated.

RNA isolation and quantification

Total RNA was extracted from cells using Trizol (Beijing Solarbio Science & Technology Co., Ltd., Beijing, China) according to the manufacturer's instructions. Next, 2 µg RNA was reverse-transcribed into cDNA. The reverse transcription-quantitative polymerase chain reaction (RT-qPCR) was performed using a SYBR kit (RR420A, Takara Bio Inc., Otsu, Shiga, Japan) and a ABI7500 qPCR instrument (Thermo Fisher Scientific Inc., Waltham, MA, USA). Three replicates were used for each treatment. All primers (Table 1) were synthesized by Shanghai Sangon Biotech (Shanghai, China). β-actin was used as an endogenous control. The fold change of gene expression was calculated using relative quantification ($2^{-\Delta\Delta Ct}$ method).

Western blot analysis

The total protein was extracted from tissues or cells. The protein concentration was determined using a bicinchoninic acid protein assay kit (Thermo Fisher Scientific Inc., Waltham, MA, USA). Next, the protein was separated by polyacrylamide gel electrophoresis at a constant voltage of 80 V for 35 min and

Table 1 Primer sequences for a reverse transcription-quantitative polymerase chain reaction.

Genes	Sequences (5′-3′)
PDLIM2	Forward: 5′-CAGCCCGCAGGGTACTTT-3′
	Reverse: 5′-GATGGGCGTGTGGAAATC-3′
β-catenin	Forward: 5′-CCAACGACTACCACCAACTTT-3′
	Reverse: 5′-GCCAGGTCTGGTTCATTGCT-3′
c-myc	Forward: 5′-TGCTCCATGAGGAGACACC-3′
	Reverse: 5′-CTTTTCCACAGAAACAACATCG-3′
CyclinD1	Forward: 5′-UGACCCCGCACGAUUUCAU-3′
	Reverse: 5′-AUGAAAUCGUGCGGGGUCA-3′
E-cadherin	Forward: 5′-TCCATTTCTTGGTCTACGCC-3′
	Reverse: 5′-CACCTTCAGCCATCCTGTTT-3′
N-cadherin	Forward: 5′-CAACTTGCCAGAAAACTCCAGG-3′
	Reverse: 5′-ATGAAACCGGGCTATCTGCTC-3′
Vimentin	Forward: 5′-ACAGTGGCCACCTACAAAGG-3′
	Reverse: 5′-CCGAGATGGGGTTGATAATG-3′
β-actin	Forward: 5′-TCACCCACACTGTGCCCATCTACGA-3′
	Reverse: 5′-CAGCGGAACCGCTCATTGCCAATGG-3′

of 120 V for 45 min and transferred onto a polyvinylidene fluoride membrane (Merck Millipore, MA, USA). After blocking with 5% skim milk for 1 h, the membrane was washed with PBS containing 0.1% Tween-20 (PBST) and incubated at 4 °C overnight with primary rabbit antibodies, phosphorylated-β-catenin (p-β-catenin) (1:300, ab27798, Abcam), β-catenin (1:1000, ab32572, Abcam), c-myc (1:1000, 5605, CST, Beverly, MA,USA), CyclinD1 (1:1000, 3300, CST, Beverly, MA, USA), GAPDH (1:5000, ab8245, Abcam), E-cadherin (1:1000, ab3195, CST, Beverly, MA, USA), and N-cadherin (1:1000, ab76057, Abcam), vimentin and Tubulin (1:1000, ab7291, Abcam) mouse antibody (1:1000, ab8978, Abcam). Next, the membranes were washed with PBST three times, 10 min per time, and incubated with horseradish peroxidase-conjugated goat anti-rabbit and goat anti-mouse secondary antibody (1:10000, Jackson, USA) at room temperature for 1 h. Following 3 PBST washes, the membranes were then immersed in enhanced chemiluminescence reaction solution (Pierce, IL, USA) at room temperature for 1 min. The liquid was removed, and the membrane was covered with food preservative film, exposed to dark environment, developed, and observed after fixation. The results were then visualized using enhanced chemiluminescence detection reagents (Thermo Fisher Scientific Inc., Waltham, MA, USA). The extraction of cytoplasmic protein was carried out using the nucleoplasmic Protein Extraction Kit (P0027, Beyotime Biotechnology, Co., Ltd., Shanghai, China) according to standard instructions, and the final protein blot images were analyzed using Image J software.

Transswell assay

The cell invasion assay was performed using a Transwell chamber (Boyden chambers; Corning, Cambridge, MA, USA). A serum-free medium was used to suspend the cells (5×10^5 cells/mL). The cell suspension was added into the Matrigel-coated (Corning, NY, USA) apical chamber of the Transwell. DMEM ($500 \mu L$) containing 10% FBS was added to the basolateral chamber of the Transwell. After incubation for 24–48 h, the cells were fixed in methanol for 20 min and stained with 0.1% Crystal Violet (Sigma-Aldrich Chemical Company, St Louis, MO, USA) for 10 min. Cells that migrated to the apical chamber were wiped out using a cotton swab. Five high-power fields (×400) were randomly selected for observation and cells were counted under an inverted microscope (Olympus, Japan).

Cell counting kit-8 (CCK-8) assay

The cells were seed into 96-well plates (Corning, NY, USA) (2000 cells/well; $100 \mu L$/well). Cells were incubated at 37 °C for 0, 1, 2, 3, and 4 days. Next, each well was added with $10 \mu L$ CCK-8 reagent (Dojindo, Kumamoto, Japan). After further incubation for 4 h, the optical density value of each well was measured at 450 nm.

Colony formation assay

Cells (800 cells per well) were seeded in 6-well plates. The medium was renewed once every two days. Next, cells were incubated with 5% CO_2 at 37 °C for 1–2 weeks. When the number of colonies grew to more than 50, the culture medium was discarded. Cells were washed with PBS and fixed with formaldehyde for 30 min. Colonies were stained with Crystal Violet for 10 min and counted.

Immunofluorescence staining

The treated cells were seeded in a 24-well plate, washed with PBS three times, fixed with 4% paraformaldehyde for 30 min, and then permeabilized with 0.5% Triton X-100 for 15 min. After washing with PBS, the cells were blocked with 10% normal goat serum for 30 min and incubated with antibodies to N-cad (1:1000, ab76057, Abcam), vimentin (1:1000, ab8978, Abcam), and PDLIM2 (1:1000, ab246868, Abcam) at 4 °C overnight. The cells were then washed with PBS, and incubated with Alexa Fluor 488 (1:400, A11001, Beijing Solarbio Science & Technology Co., Ltd., Beijing, China) or 555-coupling secondary antibody (1:400, K0032G-AF555, Beijing Solarbio Science & Technology Co., Ltd., Beijing, China) at room temperature for 1 h. The nuclei were stained with 4',6-diamidino-2-phenylindole (Vector Laboratory, Burlingame, CA, USA),

and the images were captured using a DMRA fluorescence confocal microscope (Leica, Wetzlar, German).

TOP/FOP luciferase activity test

Cells in the logarithmic growth phase were inoculated into a 96-well plate with 3 replicates for each sample. The plasmid co-transfection system was prepared and transfection was performed using Lipofectamine 2000 reagents (Catalog#12566014, Thermo Fisher Scientific Inc., Waltham, MA, USA) used according to manufacturer's instructions. After incubation for 48 h, the cells were removed, washed with PBS three times, and then lysed. The TOP/FOP luciferase activity kit (17-285, Merck-Millipore, USA) was used according to standard instructions to measure the fluorescence values.

Tumor formation in nude mice

Male BALB/c nude mice (aged 4 weeks and weighing 16–18 g) were purchased from Hunan SJA Laboratory Animal Co., Ltd. (Changsha, China). The mice were housed under standard conditions and maintained according to institutional guidelines for animal care. To establish a subcutaneous xenograft model, 2×10^6 cells (sh-PDLIM2, sh-NC, oe-PDLIM2, oe-NC) in $100 \mu L$ PBS were subcutaneously injected into the flank of mice. Tumors were removed after 4 weeks, and their size and weight were determined. The experimental metastasis model was established by injecting 4×10^6 cells treated with sh-PDLIM2, sh-NC, oe-β-catenin, oe-NC, sh-PDLIM2 + sh-β-catenin, sh-PDLIM2 + sh-NC, oe-PDLIM2 + oe-β-catenin or oe-PDLIM2 + oe-NC into the tail vein of nude mice (10 mice per group, randomly grouped in a blinded manner). After 8 weeks, metastatic tumors were imaged with the NightOWL LB983 system (Berthold Technologies, Wildbad, Germany) following D-luciferin (Promega, Madison, WI, USA) injection. The tumors were observed every 5 days after the cell injections. The longest diameter (a) and shortest length (b) of the tumor were measured using a vernier caliper and used to calculate the tumor volume (volume $= 1/2 \times L \times W^2$). After 35 days, the mice were euthanized with injection of 1% pentobarbital sodium, and the tumors were removed and weighed, followed by hematoxylin-eosin (HE) staining of the mouse lung tissues.

Statistical analysis

The SPSS 21.0 software (IBM Corp., Armonk, NY, USA) was used for all data analysis. Measurement data were summarized as mean ± standard deviation. Comparisons between two groups for data conforming to normal distribution and homogeneity of variance were analyzed using unpaired t test. Data comparisons between multiple groups were performed using one-way analysis of variance (ANOVA) with Tukey's post-hoc
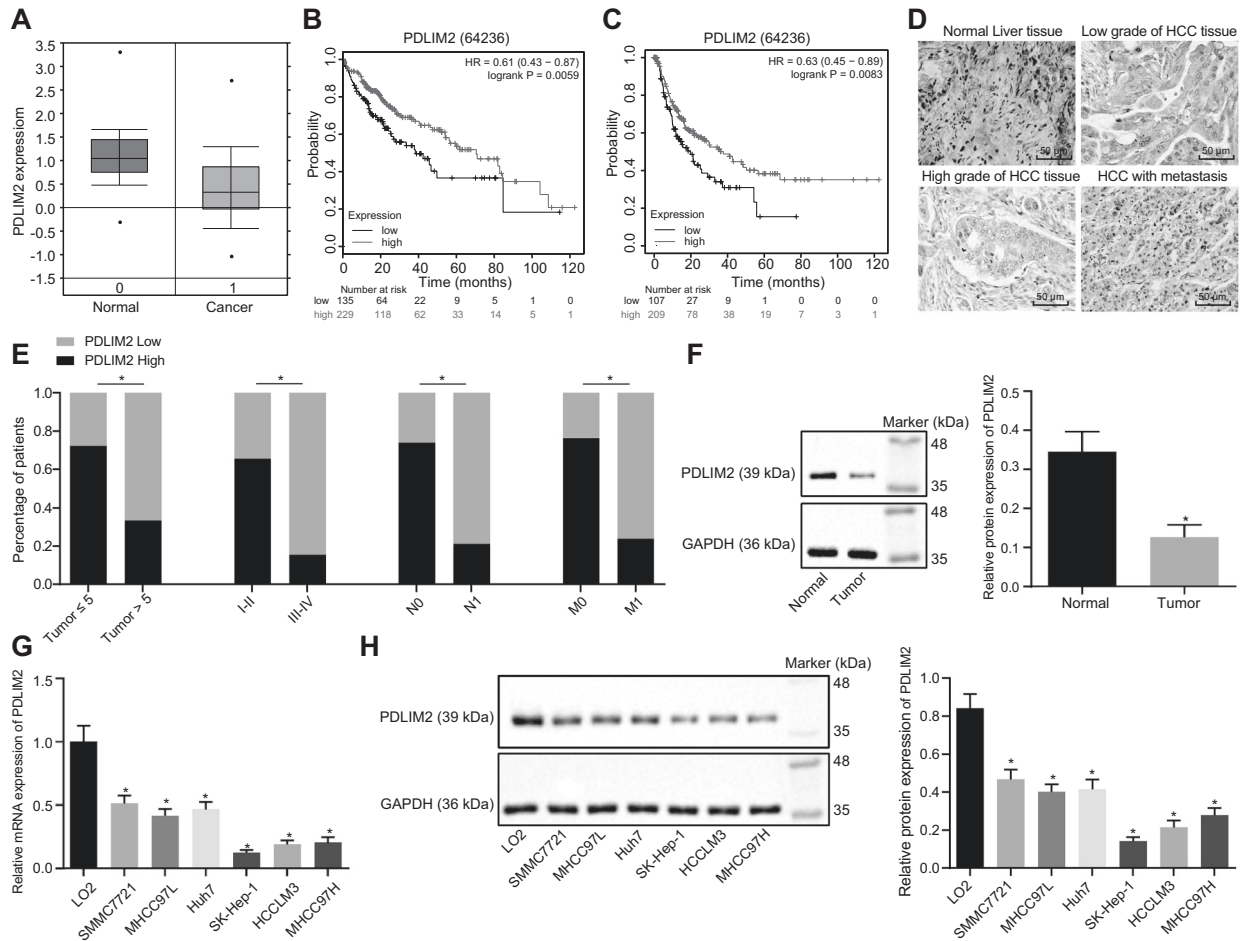
Fig. 1 PDLIM2 is downregulated in HCC tissues and cells. A PDLIM2 expression in HCC tissues and normal liver tissues analyzed using Oncomine database. * represents *p* < 0.05. **B** The relationship between PDLIM2 expression and overall survival of patients with HCC analyzed using KM-plotter. The abscissa represents the survival time, the ordinate represents the survival rate; the black line indicates the low expression sample, and the red line indicates the high expression sample. **C** The relationship between PDLIM2 expression and recurrence rate of patients with HCC analyzed using KM-plotter. The abscissa represents the survival time, and the ordinate represents the recurrence-free survival rate. **D** PDLIM2 expression in HCC tissues (*n* = 42) and normal liver tissues (*n* = 18) measured by

immunohistochemistry, scale bar = 50 μm. **E** The relationship between PDLIM2 and clinicopathological parameters in patients with HCC. **F** PDLIM2 protein level in HCC tissues (*n* = 42) and normal liver tissues (*n* = 18) measured by Western blot analysis, normalized to GAPDH. **G** PDLIM2 mRNA levels in HCC cell lines and normal liver cell lines determined using RT-qPCR, normalized to β-actin. **H** PDLIM2 protein levels in HCC cell lines and normal liver cell lines determined using Western blot analysis, normalized to GAPDH. Measurement data were summarized as mean ± standard deviation. Enumeration data were expressed as case and percentage and detected by chi-square test. * (relative to normal liver tissues or L02 cell line) indicates *p* < 0.05 by unpaired *t*-test. Cell experiments were repeated 3 times independently.

test. Data comparison between different time points was performed using repeated-measures ANOVA with Bonferroni post-hoc test. Statistical significance was set at *p* < 0.05.

Results

PDLIM2 was poorly expressed in HCC tissues and cells

Using "Oncomine", it was shown that PDLIM2 expression in HCC tissues was lower than that in normal liver tissues,

suggesting that PDLIM2 might serve as a tumor suppressor (Fig. 1A). We further analyzed the relationship between PDLIM2 and clinical prognosis of patients with HCC using 'KM-plotter' and found that low expression of PDLIM2 was associated with poor prognosis and high recurrence rate (Fig. 1B, C). In order to further explore the relationship between PDLIM2 protein expression and HCC, we selected 42 HCC tissue samples and 18 normal liver tissue samples to determine the PDLIM2 expression using immunohistochemistry and Western blot analysis. The findings revealed that PDLIM2 protein level was lower in HCC tissues as compared to control, and PDLIM2 expression was

negatively associated with tumor size, stage, and lymph node metastasis (Fig. 1D-F). To further study the effect of PDLIM2 on HCC cells, we selected the normal liver cell line HL7702 (L02) and HCC cell lines SMMC7721, MHCC97L, Huh7, SMMC7721, SK-Hep1, HCCLM3, and MHCC97H for quantification of PDLIM2 expression. Western blot analysis and RT-qPCR displayed that PDLIM2 levels were significantly diminished in HCC cell lines when compared with the normal liver cell lines. Moreover, PDLIM2 levels in highly metastatic HCC cell lines, SK-Hep-1, HCCLM3, and MHCC97H cells were lower than those in cell lines with low metastatic potential, SMMC7721, MHCC97L, and Huh7 cells (Fig. 1G, H). Therefore, the SMMC7721 and Huh7 cell lines with low metastatic potential, and HCCLM3 and SK-Hep-1 with high metastatic potential were selected for the subsequent experiments. These findings suggested that poorly expressed PDLIM2 was correlated with metastasis and poor prognosis of HCC.

PDLIM2 inhibited the proliferation and growth of HCC cells both in vitro and in vivo

In order to study the effect of PDLIM2 on the proliferation and tumorigenicity of HCC cells, SMMC7721 and Huh7 cell lines with low invasiveness and HCCLM3 and SK-Hep-1 cell lines with high invasiveness were used for the construction of cell lines with stable PDLIM2 knockdown and PDLIM2 overexpression, respectively (Supplementary Figure 1A-B). The CCK-8 assay and colony formation assay showed accentuated cell growth and colony formation ability in the SMMC7721 and Huh7 cells treated with shRNA targeting PDLIM2, whereas the opposing results were noted in the HCCLM3 and SK-Hep-1 cells treated with expression vectors containing PDLIM2 (Fig. 2A, B). Next, we constructed xenograft models of nude mice to observe the effect of PDLIM2 in vivo. Nude mice injected with SMMC7721-sh-PDLIM2 displayed increased tumor size and volume along with higher Ki-67 and PDLIM2 expression, while nude mice injected with HCCLM3-PDLIM2 showed decreased tumor size and volume and lower Ki-67 and PDLIM2 expression (Fig. 2C, Supplementary Fig. 2). These findings demonstrated that PDLIM2 inhibited the proliferation and growth of HCC cells both in vitro and in vivo.

PDLIM2 inhibited the migration, invasion and metastasis of HCC cells

Next, the focus of our study was the influence of PDLIM2 on the migration and invasion of HCC cells in vitro. Wound healing assay and Transwell assay displayed that cell migration and invasion were enhanced in SMMC7721 and Huh7 cells treated with shRNA targeting PDLIM2, but inhibited in HCCLM3 and SK-Hep-1 cells treated with expression vectors containing PDLIM2 (Fig. 3A, B). Nude mice were injected with the transfected cell lines (SMMC7721-sh-PDLIM2 and HCCLM3-PDLIM2) via the tail vein and monitored for the development of pulmonary metastatic nodules, in order to evaluate the role of PDLIM2 in tumor metastasis in vivo. The nude mice injected with SMMC7721-sh-PDLIM2 displayed higher numbers and larger sized pulmonary metastatic nodules, while those injected with HCCLM3-PDLIM2 showed fewer and smaller pulmonary metastatic nodules (Fig. 3C, Supplementary Fig. 3). HE staining confirmed the presence of metastatic nodules in the lung tissues (Fig. 3D). These findings implied that PDLIM2 inhibited the migration, invasion, and metastasis of HCC cells.

PDLIM2 was mainly localized in the cytoplasm of HCC cells

Immunohistochemistry depicted PDLIM2 was mainly localized in the nucleus in normal liver tissues but as the disease progressed, PDLIM2 was mainly expressed in the cytoplasm/membrane, and not expressed in the nucleus of tumor cells (Fig. 4A, Supplementary Figure 1C). Similarly, the quantification of PDLIM2 staining in cytoplasm/membrane versus that in the nucleus showed that it was only expressed in cytoplasm/membrane area in HCC cells (Fig. 4B) in contrast to the high level of nuclear PDLIM2 seen in normal liver cells.

PDLIM2 inhibited β-catenin activity and downstream gene expression

Subsequently, the regulatory effects of PDLIM2 on β-catenin and its downstream genes were investigated. Western blot analysis showed that PDLIM2 upregulation inhibited β-catenin expression and its activity in HCCLM3 cells, whereas PDLIM2 knockdown led to the opposite results in SMMC7721 cells (Fig. 5A, B). TOP/FOP luciferase activity test demonstrated that upregulated PDLIM2 in HCCLM3 and SK-Hep-1 cells inhibited the promoter activity of β-catenin, while the opposing results were found in SMMC7721 and Huh7 cells treated with shRNA targeting PDLIM2 (Fig. 5C, D). Western blot analysis and RT-qPCR showed that c-myc and cyclinD1 reduced in HCCLM3 and SK-Hep-1 cells treated with expression vectors containing PDLIM2, while they were raised in SMMC7721 and Huh7 cells treated with shRNA targeting PDLIM2 (Fig. 5E–H). These data indicated that PDLIM2 facilitated the inhibition of β-catenin activity and its downstream gene expression.
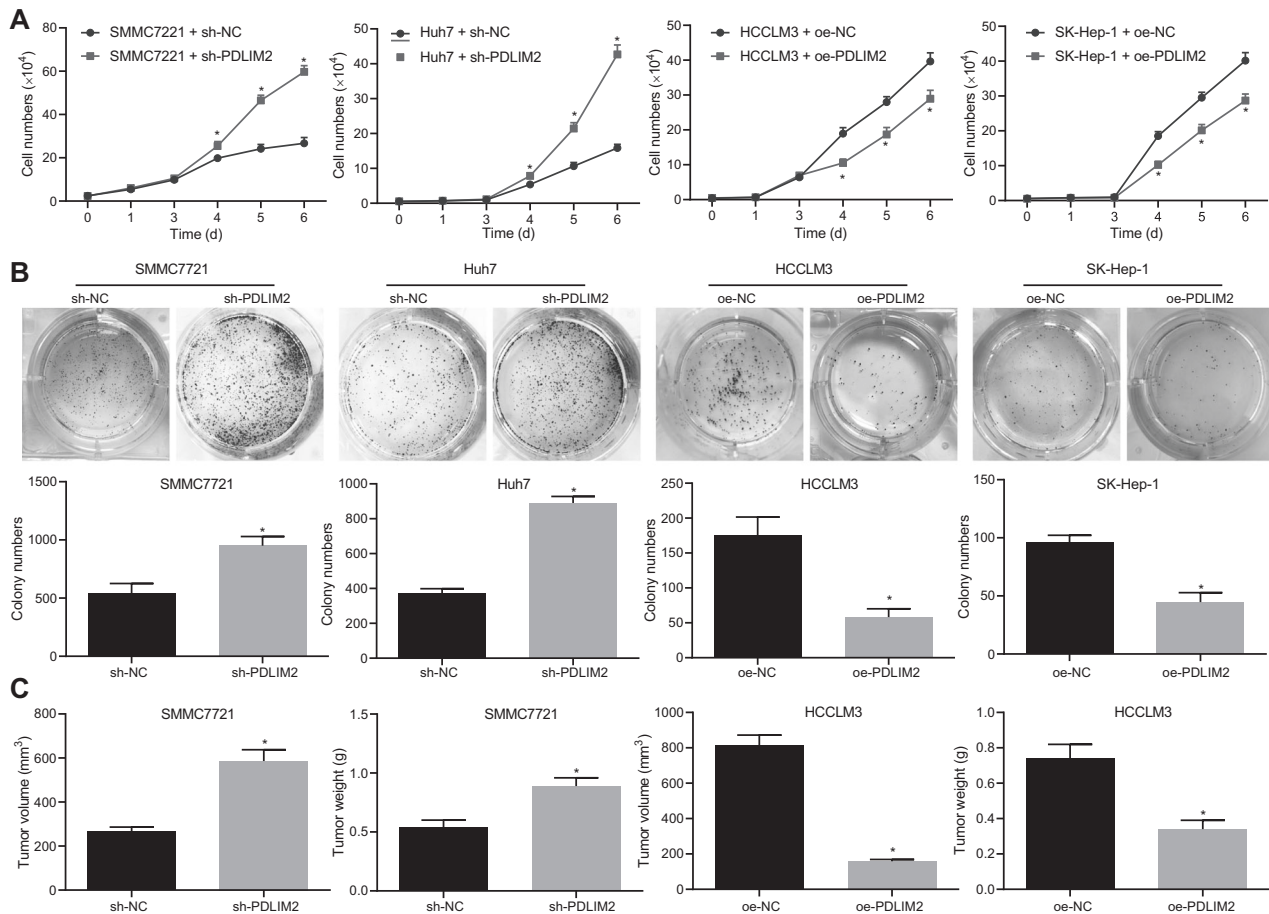
Fig. 2 PDLIM2 suppresses the proliferation and growth of HCC cells both in vitro and in vivo. SMMC7721 and Huh7 cells were treated with shRNA targeting PDLIM2, and HCCLM3 and SK-Hep-1 cells were treated with expression vectors containing PDLIM2. **A** Cell growth curve plotted based on CCK-8 assay. **B** Representative images and quantitative analysis showing colony formation ability of HCC cells. Xenograft model nude mice ($n = 10$ in each group) were injected with SMMC7721-sh-PDLIM2 and HCCLM3-PDLIM2. **C** Quantitative analysis of volume and weight of the tumors of HCC cells in nude mice. Measurement data were summarized as mean ± standard deviation. * (relative to cells treated with sh-NC or oe-NC) indicates $p < 0.05$ by unpaired t test. Cell experiments were repeated 3 times independently.

PDLIM2 inhibited the EMT of HCC cells and lung metastasis by regulating β-catenin

Western blot analysis revealed that SMMC7721 cells treated with shRNA targeting PDLIM2 downregulated the expression of E-cadherin and zonula occludens-1 and upregulated expression of N-cadherin and vimentin, whereas the opposite findings were evident in HCCLM3 treated with expression vectors containing oe-PDLIM2 (Fig. 6A). The immunofluorescence staining results (Supplementary Figure 4A) were consistent with these findings. The above results confirmed that PDLIM2 could further inhibit cell migration and invasion in HCC by inhibiting EMT.

Next, HCCLM3 cells were treated with expression vectors for PDLIM2 and β-catenin, while SMMC7721 cells were treated with shRNA targeting PDLIM2 and β-catenin. Western blot analysis showed that β-catenin knockdown rescued the reduction of E-cadherin and the elevation of vimentin induced by PDLIM2 downregulation (Fig. 6B), which was further confirmed by the immunofluorescence staining (Supplementary Figure 4B). Moreover, β-catenin knockdown counterweighed the promoting effect of PDLIM2 downregulation on the migration and invasion of SMMC7721 cells, while elevated β-catenin reversed the PDLIM2-induced inhibition of migration and invasion of HCCLM3 cells (Fig. 6C).

To explore if PDLIM2 regulates lung metastasis in HCC in vivo by affecting β-catenin, we next generated a lung metastatic colonization model by inoculating HCCLM3 cells or SMMC7721 cells into the tail veins of mice. The incidence of lung metastasis in each group was determined by observing the lung tissue dissection and HE staining. As shown in Fig. 6D and Supplementary Figure 4C, silencing PDLIM2 increased the number of pulmonary metastases, which was reversed by knockdown of β-catenin. The
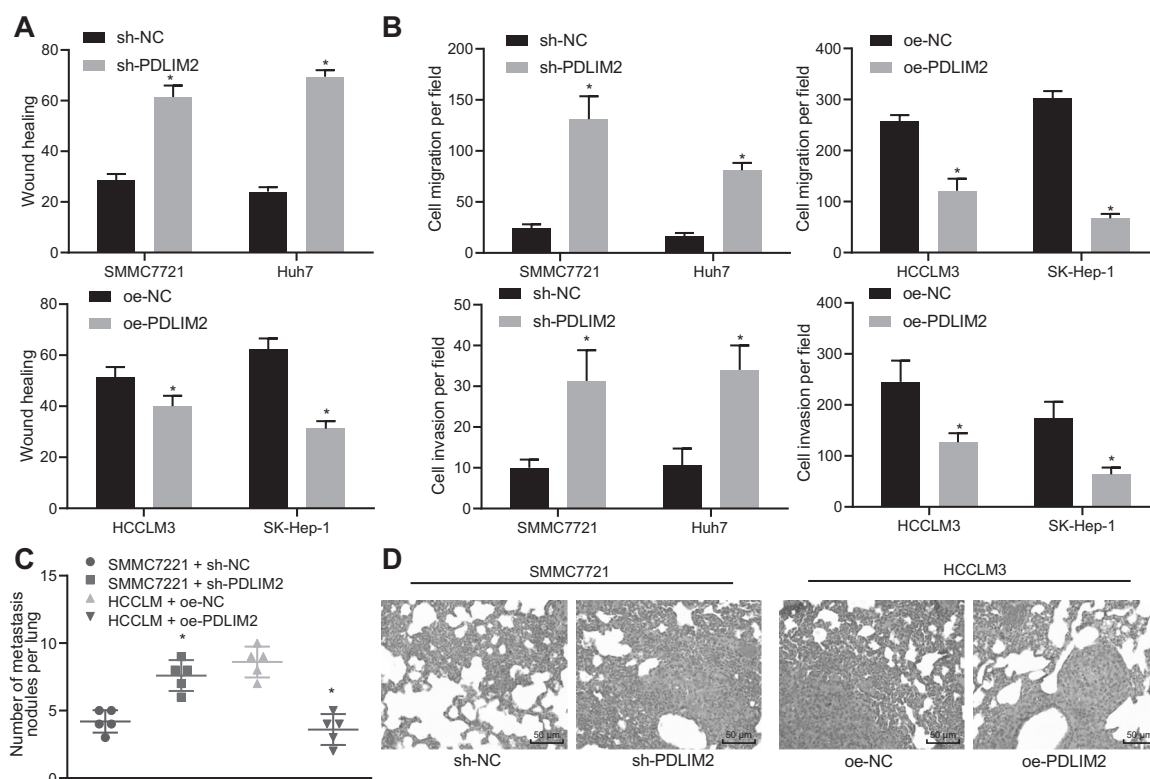
Fig. 3 PDLIM2 suppresses migration, invasion, and metastasis of hepatocellular carcinoma (HCC) cells. A Cell migration detected by wound healing assay. **B** Cell migration and invasion detected by transwell assay. Xenograft model nude mice ($n = 10$ in each group) were injected with SMMC7721-shPDLIM2 and HCCLM3-PDLIM2. **C** Quantitative analysis of pulmonary metastatic nodules. **D** Pathological characteristics of lung tissues detected by HE staining, scale bar = 50 μm. Measurement data were summarized as mean ± standard deviation. *(relative to cells treated with sh-NC or oe-NC) *p < 0.05 by unpaired t test. Cell experiments were repeated three times independently.
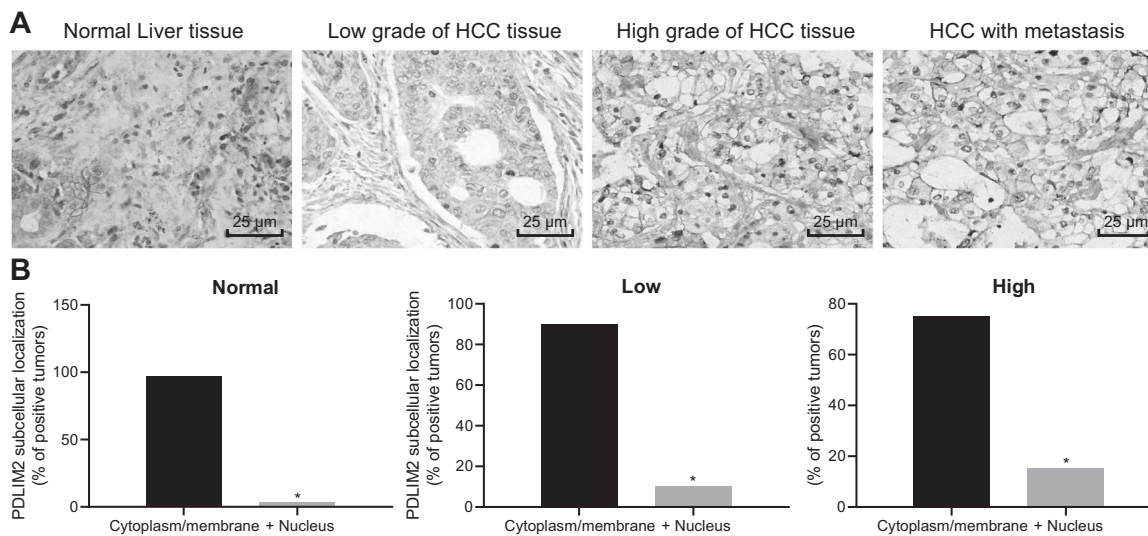

Fig. 4 PDLIM2 is mainly localized in the cytoplasm of HCC cells. A Localization of PDLIM2 in normal liver tissues and HCC tissues during different stages by immunohistochemistry, scale bar = 25 μm. **B** Quantification of PDLIM2 in normal liver and HCC tissues during different stages by Image J. Measurement data were summarized as mean ± standard deviation. * (relative to Cytoplasm/membrane) indicates p < 0.05. Cell experiments were repeated 3 times independently.
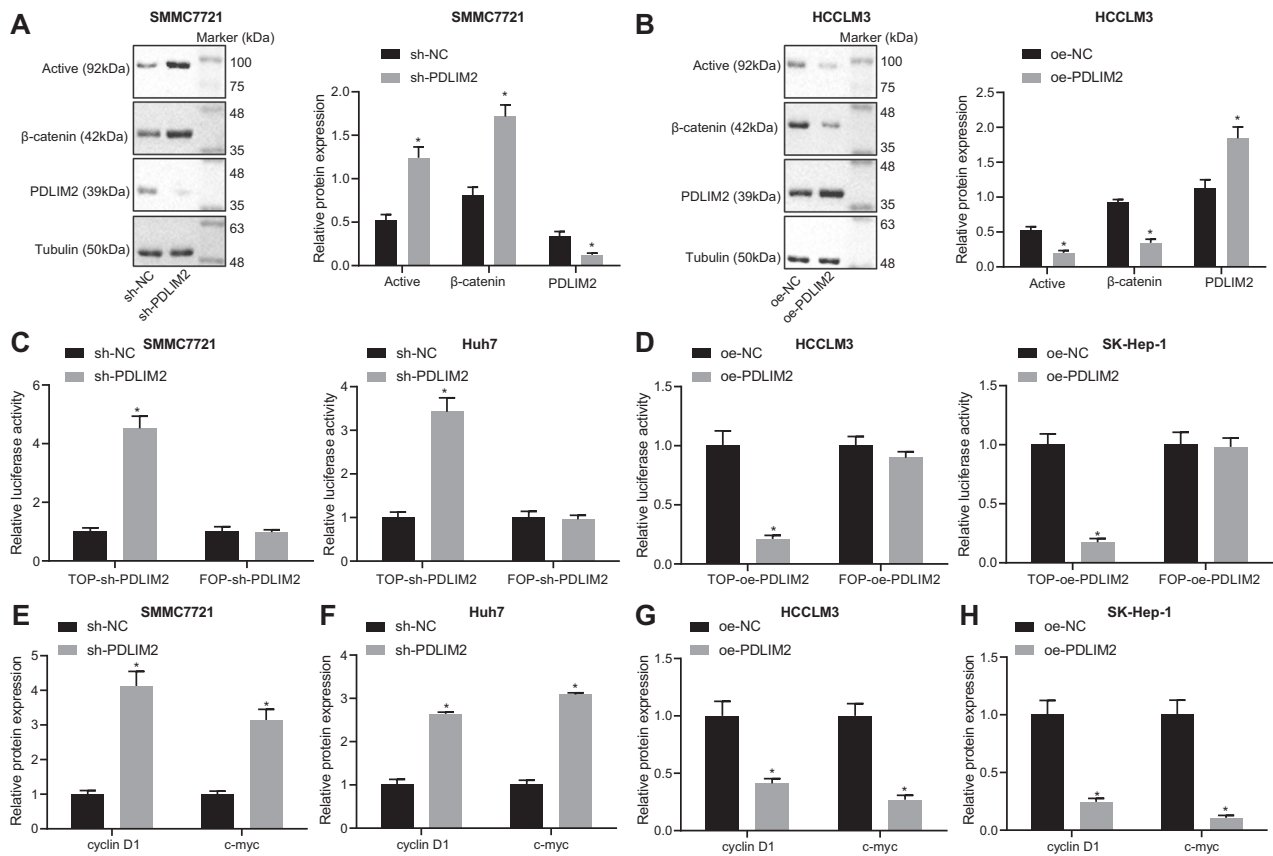
Fig. 5 PDLIM2 suppresses β-catenin activity and downstream gene expression. SMMC7721 and Huh7 cells were treated with shRNA targeting PDLIM2, and, HCCLM3 and SK-Hep-1 cells were treated with expression vectors containing PDLIM2. **A** Immunoblots of β-catenin activity and PDLIM2, and quantitative analysis of β-catenin protein expression in response to PDLIM2 knockdown in SMMC7721 cells. **B** Immunoblots of β-catenin activity and PDLIM2, and quantitative analysis of β-catenin protein expression in response to PDLIM2 overexpression in HCCLM3 cells. **C** The promoter activity of β-catenin in response to PDLIM2 knockdown in SMMC7721 and Huh7 cells detected by TOP/FOP luciferase activity test. **D** The promoter activity of β-catenin in response to PDLIM2 overexpression in HCCLM3 and SK-Hep-1 cells detected by TOP/FOP luciferase activity test. **E, F** Quantitative analysis of protein levels of c-myc and cyclinD1 in response to PDLIM2 knockdown in SMMC7721 and Huh7 cells as determined using Western blot analysis, normalized to GAPDH. **G, H** Quantitative analysis of protein levels of c-myc and cyclinD1 in response to PDLIM2 overexpression in HCCLM3 and SK-Hep-1 cells as determined using Western blot analysis, normalized to GAPDH. Measurement data were summarized as mean ± standard deviation. * (relative to cells treated with sh-NC or oe-NC) indicates $p < 0.05$ by unpaired t test. Cell experiments were repeated 3 times independently.

reverse effect was observed in the presence of simultaneous overexpression of PDLIM2 and β-catenin. It was thus concluded that β-catenin was a downstream effector of PDLIM2-mediated inhibition of HCC cell invasion and metastasis

Discussion

Currently, only 30–40% of patients with HCC are amenable to curative resection owing to the late onset of symptoms, and prognosis remains poor due to the high frequency of metastasis and recurrence [14]. These challenges suggest an urgent need to identify potential molecules that can be leveraged for diagnosing, predicting, and treating early and late recurrences and metastases, and in particular,

identifying the patients with a high risk of early recurrence and metastasis [15]. In the present study, PDLIM2 and β-catenin expression were altered in HCC cells and in vivo mouse models to explore the effects of PDLIM2 and β-catenin on cell proliferation, migration, invasion, and EMT. Taken together, our findings provided evidence demonstrating that upregulation of PDLIM2 repressed β-catenin expression, thus suppressing the cancer cell proliferation, migration, invasion, and EMT, which consequently attenuated HCC progression.

Our initial results showed that PDLIM2 was poorly expressed in HCC tissues and cells, and low PDLIM2 expression was found correlated with worse prognosis in HCC patients. Importantly, PDLIM2 reduced the levels of N-cadherin and vimentin and elevated levels of E-cadherin and zonula occludens-1, which corroborated with inhibited
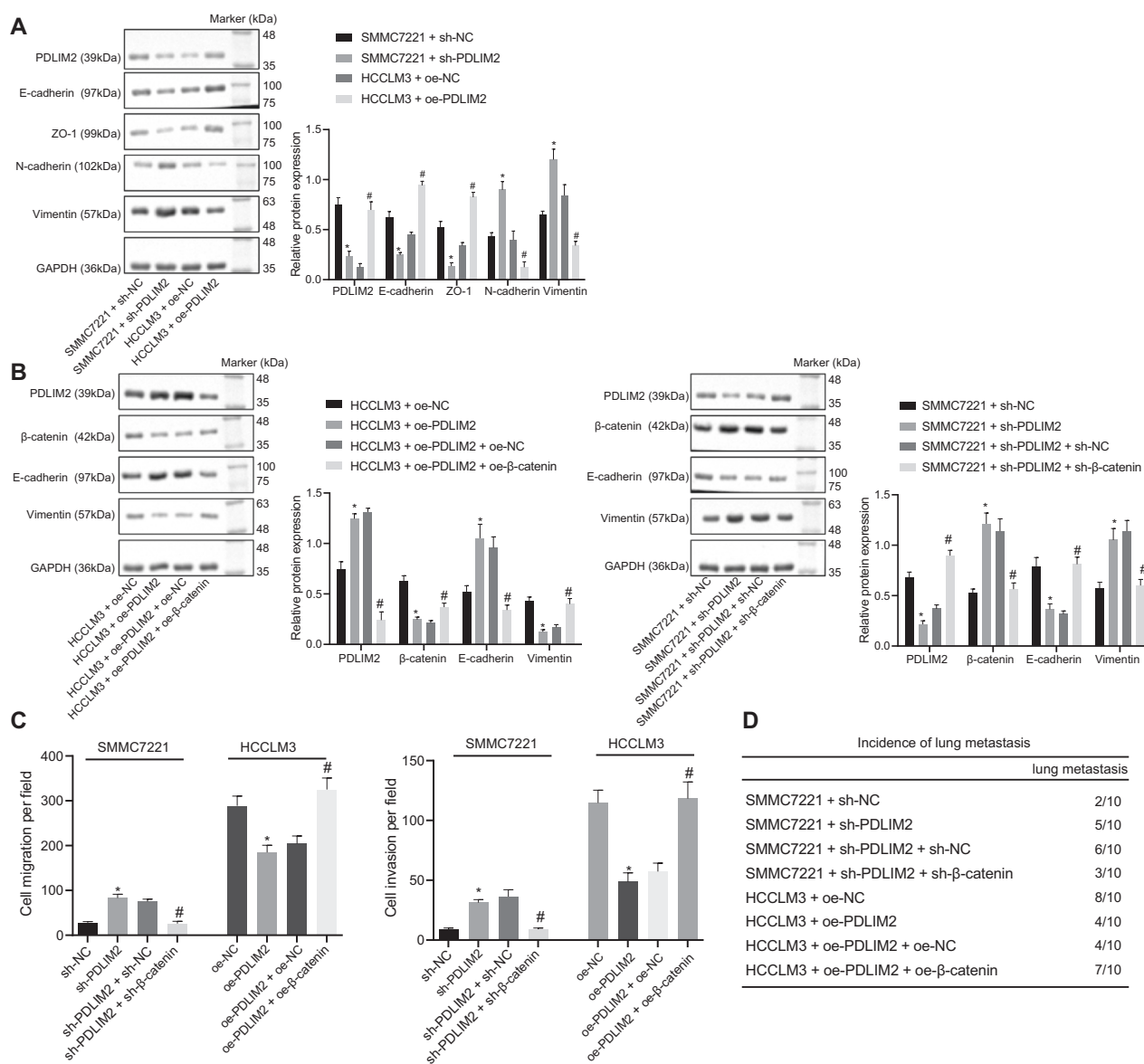
Fig. 6 PDLIM2 suppresses EMT in HCC cells and lung metastasis by regulating β-catenin. SMMC7721 cells were treated with shRNA targeting PDLIM2, and HCCLM3 cells were treated with expression vectors containing PDLIM2. **A** Protein levels of PDLIM2, E-cadherin, zonula occludens-1, N-cadherin, and vimentin in SMMC7721 and HCCLM3 cells determined using Western blot analysis, normalized to GAPDH. **B** Protein levels of PDLIM2, E-cadherin, zonula occludens-1, N-cadherin, and vimentin in SMMC7721 cells and HCCLM3 cells determined using Western blot analysis, normalized to GAPDH. **C** Quantitative analysis of cell migration and invasion ability of SMMC7721 cells and HCCLM3 cells detected by Transwell assay. Xenograft model nude mice ($n = 10$ in each group) were injected with HCCLM3 cells treated with expression vectors containing PDLIM2 and β-catenin, and, SMMC7721 cells treated with shRNA targeting PDLIM2 and β-catenin. **D** Quantitative analysis of pulmonary metastatic nodules. Measurement data were summarized as mean ± standard deviation. * (relative to cells treated with sh-NC or oe-NC) indicates $p < 0.05$ by unpaired t test. Cell experiments were repeated 3 times independently.

HCC cell proliferation, migration, invasion, and EMT both in vitro and in vivo. EMT is a critical process involved in cancer progression and the acquisition of invasive characteristics of the tumor is closely related to invasion and metastasis in HCC [3]. Increased cell motility and invasion are recognized to have a positive correlation with EMT, which is characterized by repression of epithelial markers such as E-cadherin and induction of mesenchymal markers such as N-cadherin and vimentin [16]. PDLIM2 is the most recently discovered PDZ-LIM domain-containing protein, which can bind to the actin cytoskeleton and is thus implicated in both normal development and disease [17]. PDLIM2 has been reported to be inhibited epigenetically in several human cancers [7]. The mRNA levels of PDLIM2 were detected to be highly downregulated in colorectal cancer tissues compared to normal tissues [8]. Qu et al.

found PDLIM2 expression was repressed in colon cancer tissues and cells, and its elevation suppressed tumor growth and tumor formation in colon cancer in vitro and in vivo, which supports a tumor suppressor role of PDLIM2 [9]. Others have noted PDLIM2, implicated in EMT and immune response, was downregulated in metastatic tumors, suggesting its potential role in altered immune signaling [8]. PDLIM2 has also been identified to promote EMT by regulating the stability of transcription factors including NF-κB and STATs [18]. This differs from the present findings, which may be the difference of the laboratory environment, study subjects, and the detection methods used. Therefore, it could be concluded that PDLIM2 exhibited anti-oncogenic activities in HCC, and thus, we explored the relevant underlying mechanisms.

We showed that PDLIM2 inhibited β-catenin activity and its downstream gene expressions, such as c-myc and cyclinD1. Inhibition of the β-catenin signaling pathway has the potency to delay the progression of colorectal cancer [19]. Given the anti-cancer property of PDLIM2 in colorectal cancer [9], we reasoned that PDLIM2 could cause a decline of β-catenin expression. Similar to our findings, PDLIM2 has been identified to be a key regulator of cancer-associated genes including the proto-oncogene c-myc [8]. CyclinD1 and c-myc are reported to be downstream target genes of β-catenin [10]. PDLIM2 has been signified to prevent human auto-immune disease by restricting expression of Th1 and Th17 cytokines [20]. Meanwhile, Wnt-10b, a member of the Wnt/β-catenin pathway, was increased in the synovial membrane of rats with rheumatoid arthritis [21]. Furthermore, TCF7L2 (also known as Tcf-4), a Wnt transcription factor, contributes to HCC progression [22]. Thus, an adverse correlation could be obtained between PDLIM2 and the Wnt/β-catenin pathway. Furthermore, our findings revealed that β-catenin knockdown rescued the reduction of E-cadherin and the elevation of vimentin expression induced by PDLIM2 downregulation, thereby suppressing cell proliferation, migration, invasion, and EMT to repress the progression of HCC. β-catenin is of great significance to all phases of liver development and maturation, and the aberrant activation of β-catenin is an important mechanistic event during the development of HCC [23]. Importantly, β-catenin has been noted to reduce E-cadherin levels [11], implying its effect on EMT. In agreement, a recent study found that β-catenin induced by downregulated miR-200a promoted EMT in HCC, thus promoting tumorigenicity [24], which suggested that the silencing of β-catenin might inhibit EMT and thereby suppress HCC progression. Meanwhile, activating the Wnt/β-catenin pathway helps to promote HCC cell migration, invasion, growth, and metastasis in vitro [25]. Taken together with previous evidence, our results validated that PDLIM2 inhibited the cell proliferation, migration, invasion, and EMT in HCC by downregulating β-catenin.
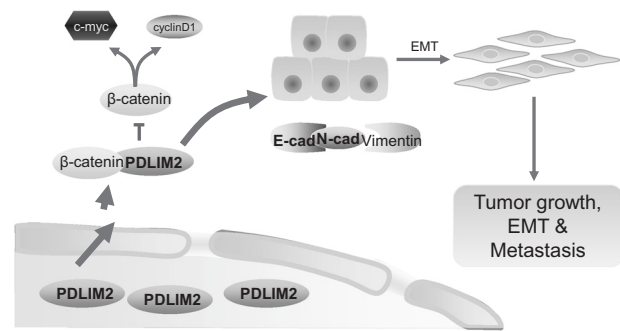

Fig. 7 Role of PDLIM2 in the development and epithelial-mesenchymal transition (EMT) of hepatocellular carcinoma (HCC) by regulating β-catenin. Translation of PDLIM2 into nuclei can inhibit the activation of β-catenin, thereby reversing EMT in HCC cells and inhibiting cell proliferation, migration, and invasion.

In conclusion, our study demonstrated that upregulation of PDLIM2 could inhibit the expression of β-catenin, which potentially suppressed cell proliferation, migration, invasion, and EMT and thus repressed the progression of HCC (Fig. 7). Our study also provided further insight into the regulatory network and the mechanistic role of PDLIM2 in regulating β-catenin expression in HCC. However, further investigations are imperative to evaluate the possibilities of clinical translation of these results. In addition, more research is warranted to comprehensively characterize all possible mechanisms by which PDLIM2 interacts with β-catenin and influences HCC progression.

Author contributions Xiaoming Jiang and Ying Tang designed the study. Zhe Chu was involved in data collection. Yang Cao and Ying Shi performed the statistical analysis and preparation of figures. Ying Tang and Xu Shi drafted the paper. All authors read and approved the final manuscript.

Compliance with ethical standards

Conflict of interest The authors declare that they have no conflict of interest.

Publisher's note Springer Nature remains neutral with regard to jurisdictional claims in published maps and institutional affiliations.

References

1. Caruso S, Nault JC. A dive into the deep heterogeneity of hepatocellular carcinoma. Gastroenterology. 2019;157:1477–9.
2. Cui H, Zhang Y, Zhang Q, Chen W, Zhao H, Liang J. A comprehensive genome-wide analysis of long noncoding RNA

expression profile in hepatocellular carcinoma. Cancer Med 2017;6:2932–41.

3. He P, Zhang HX, Sun CY, Chen CY, Jiang HQ. Overexpression of SASH1 inhibits the proliferation, invasion, and EMT in hepatocarcinoma cells. Oncol Res. 2016;24:25–32.

4. Pinto Marques H, Gomes da Silva S, De Martin E, Agopian VG, Martins PN. Emerging biomarkers in HCC patients: Current status. Int J Surg. 2020. https://doi.org/10.1016/j.ijsu.2020.04.043.

5. Ding GY, Zhu XD, Ji Y, Shi GM, Shen YH, Zhou J, et al. Serum PON1 as a biomarker for the estimation of microvascular invasion in hepatocellular carcinoma. Ann Transl Med. 2020;8:204.

6. Tanaka T, Grusby MJ, Kaisho T. PDLIM2-mediated termination of transcription factor NF-kappaB activation by intranuclear sequestration and degradation of the p65 subunit. Nat Immunol. 2007;8:584–91.

7. Sun F, Xiao Y, Qu Z. Oncovirus Kaposi sarcoma herpesvirus (KSHV) represses tumor suppressor PDLIM2 to persistently activate nuclear factor kappa B (NF-kappaB) and STAT3 transcription factors for tumorigenesis and tumor maintenance. J Biol Chem. 2015;290:7362–8.

8. Oh BY, Cho J, Hong HK, Bae JS, Park WY, Joung JG, et al. Exome and transcriptome sequencing identifies loss of PDLIM2 in metastatic colorectal cancers. Cancer Manag Res. 2017;9:581–9.

9. Qu Z, Yan P, Fu J, Jiang J, Grusby MJ, Smithgall TE, et al. DNA methylation-dependent repression of PDZ-LIM domain-containing protein 2 in colon cancer and its role as a potential therapeutic target. Cancer Res. 2010;70:1766–72.

10. Fatima S, Shi X, Lin Z, Chen GQ, Pan XH, Wu JC, et al. 5-Hydroxytryptamine promotes hepatocellular carcinoma proliferation by influencing beta-catenin. Mol Oncol. 2016;10:195–212.

11. Lai TY, Su CC, Kuo WW, Yeh YL, Kuo WH, Tsai FJ, et al. beta-catenin plays a key role in metastasis of human hepatocellular carcinoma. Oncol Rep. 2011;26:415–22.

12. Anson M, Crain-Denoyelle AM, Baud V, Chereau F, Gougelet A, Terris B, et al. Oncogenic beta-catenin triggers an inflammatory response that determines the aggressiveness of hepatocellular carcinoma in mice. J Clin Invest. 2012;122:586–99.

13. Sun L, Liu T, Zhang S, Guo K, Liu Y. Oct4 induces EMT through LEF1/beta-catenin dependent WNT signaling pathway in hepatocellular carcinoma. Oncol Lett. 2017;13:2599–606.

14. Han D, Li J, Wang H, Su X, Hou J, Gu Y, et al. Circular RNA circMTO1 acts as the sponge of microRNA-9 to suppress hepatocellular carcinoma progression. Hepatology 2017;66:1151–64.

15. Xu B, Cai Z, Zeng Y, Chen L, Du X, Huang A, et al. alpha-Methylacyl-CoA racemase (AMACR) serves as a prognostic biomarker for the early recurrence/metastasis of HCC. J Clin Pathol. 2014;67:974–9.

16. Wu S, Du R, Gao C, Kang J, Wen J, Sun T. The role of XBP1s in the metastasis and prognosis of hepatocellular carcinoma. Biochem Biophys Res Commun. 2018;500:530–7.

17. Torrado M, Senatorov VV, Trivedi R, Fariss RN, Tomarev SIP-dlim2. a novel PDZ-LIM domain protein, interacts with alpha-actinins and filamin A. Invest Ophthalmol Vis Sci. 2004;45:3955–63.

18. Cox OT, O'Shea S, Tresse E, Bustamante-Garrido M, Kiran-Deevi R, O'Connor R. IGF-1 receptor and adhesion signaling: an important axis in determining cancer cell phenotype and therapy resistance. Front Endocrinol (Lausanne). 2015;6:106.

19. Cheng X, Xu X, Chen D, Zhao F, Wang W. Therapeutic potential of targeting the Wnt/beta-catenin signaling pathway in colorectal cancer. Biomed Pharmacother. 2019;110:473–81.

20. Qu Z, Fu J, Ma H, Zhou J, Jin M, Mapara MY, et al. PDLIM2 restricts Th1 and Th17 differentiation and prevents autoimmune disease. Cell Biosci. 2012;2:23.

21. de Sousa LM, Dos Santos Alves JM, da Silva Martins C, Pereira KMA, Goes P, Gondim DV. Immunoexpression of canonical Wnt and NF-kappaB signaling pathways in the temporomandibular joint of arthritic rats. Inflamm Res. 2019;68:889–900.

22. Li C, Wu W, Ding H, Li Q, Xie K. The transcription factor 7 like 2binding protein TIP5 activates betacatenin/transcription factor signaling in hepatocellular carcinoma. Mol Med Rep. 2018;17:7645–51.

23. Li ZQ, Ding W, Sun SJ, Li J, Pan J, Zhao C, et al. Cyr61/CCN1 is regulated by Wnt/beta-catenin signaling and plays an important role in the progression of hepatocellular carcinoma. PLoS ONE. 2012;7:e35754.

24. Liu J, Ruan B, You N, Huang Q, Liu W, Dang Z, et al. Down-regulation of miR-200a induces EMT phenotypes and CSC-like signatures through targeting the beta-catenin pathway in hepatic oval cells. PLoS ONE. 2013;8:e79409.

25. Zhang T, Ma Z, Liu L, Sun J, Tang H, Zhang B, et al. DDX39 promotes hepatocellular carcinoma growth and metastasis through activating Wnt/beta-catenin pathway. Cell Death Dis. 2018;9:675.